

Shocks in non-loaded bead chains with impurities

Erwan Hascoët¹ and Hans J. Herrmann^{1,2}

March 5, 2018

¹P.M.M.H. Ecole Supérieure de Physique et Chimie Industrielles,
10, rue Vauquelin, 75231 Paris CEDEX 05 France

²ICA1, University of Stuttgart, Pfaffenwaldring 27, D-70569 Stuttgart Germany

Abstract

We numerically investigate the problem of the propagation of a shock in an horizontal non-loaded granular chain with a bead interaction force exponent varying from unity to large values. When α is close to unity we observed a cross-over between a nonlinearity-dominated regime and a solitonic one, the latest being the final steady state of the propagating wave. In the case of large values of α the deformation field given by the numerical simulations is completely different from the one obtained by analytical calculation. In the following we studied the interaction of these shock waves with a mass impurity placed in the bead chain. Two different physical pictures emerge whether we consider a light or a heavy impurity mass. The scatter of the shock wave with a light impurity yields damped oscillations of the impurity which then behave as a solitary wave source. Differently an heavy impurity is just shifted by the shock and the transmitted wave loses its solitonic character being fragmented into waves of decreasing amplitudes.

1 Introduction

Since the pioneering work of Nesterenko [1] there has been an increase of activity devoted to the study of wave propagation in granular media. The theoretical prediction of solitons-like waves propagating in one dimensional chains of perfect elastic spheres has been experimentally checked by Lazaridi and Nesterenko [2] and more recently by Coste, Falcon and Fauve [3]. These studies concern the idealized case of spheres interacting according to the Hertz law where the interaction force depends on the overlap distance of the spheres to the power $\frac{3}{2}$. The result of Nesterenko for the particular Hertzian case can actually be generalized to an interaction law where the exponent can vary from one to infinity [4], the

case of the exponent equal to unity being special since it leads to a self-similar asymmetric pulse propagation resulting from a shock perturbation [5, 6]. Instead of traveling as a soliton the pulse propagates increasing its width and decreasing its amplitude. It was then showed that the amplitude decreases like $t^{-0.17}$ and the width increases like $t^{\frac{1}{3}}$. This generalization of the interaction law by letting the interaction exponent vary allows us to take into account the various shapes of two interacting beads.

Besides isolating non-linearities in one dimensional chains other physical ingredients have been added in order to make these models more realistic. Sinkovits and Sen [7] did molecular dynamics simulations on gravitationally compacted Hertzian chains. It was then observed that gravitation makes waves lose their soliton-like features becoming solitary waves with the wave speed increasing with depth z as $z^{\frac{1}{6}}$ as predicted by Hertz law. Besides, if an impurity is placed in the chain, the propagating wave is scattered by it and a reflected wave is obtained in addition to the transmitted wave, these waves having a similar shape as the incident wave. Following these first results Hong, Ji and Kim [8] extracted several power laws for the velocity amplitude of a wave propagating in a gravitationally compacted chain. It was shown that in a homogeneous chain of beads the amplitude velocity of the solitary pulse decreases like $z^{-\frac{1}{4}(\frac{1}{3}+\frac{1}{\alpha})}$ for an interaction law exponent α greater than unity. This power law is only valid in the case of a small perturbation where the non-linear interaction law can be locally linearized, the stiffness coefficient then varying with depth.

In this paper, we present molecular dynamics results for non-loaded horizontal granular chains containing impurities. In our model the force interaction law exponent is allowed to vary from one to infinity, the Hertzian case being considered as a special one. After having reviewed the theoretical results for shock propagation in a horizontal bead chain and their relevance in reproducing the results from numerical simulations we study the interaction of shock waves with impurities of various masses. We show that the patterns observed for the scattered waves vary as impurity masses are larger or smaller than the mass of the beads constituting the granular chain. In the case of a light impurity we observed a backscattered solitary wave followed by an increasing number of secondary waves of decreasing amplitudes produced at the impurity location. These secondary waves also propagate in the forward direction following the transmitted wave. We looked at the displacement of the impurity after the collision. The impurity actually oscillates in a ballistic motion around its equilibrium position. These oscillations are damped since the impurity collides its nearest neighbors producing a backward and a forward moving pulse in each cycle. If we consider the interaction of a shock with an heavy impurity we obtain a very different scenario. Instead of exciting the impurity the shock only shifts it in its moving direction. The chain is then halved in two separated chains on which propagate several pulses. The situation is no more symmetric as in the previous case. After the collision the incident wave does not produce a stable transmitted wave but is decomposed in

a series of pulses of decreasing amplitudes. Before the impurity we observe the propagation of a stable reflected solitary wave. In each case the amplitude of the reflected pulse grows with the absolute value of the difference between the mass of the impurity and the normal mass. Hence the speed of the reflected pulse grows with this mass difference since the speed of our solitary waves increases with the amplitude.

In section 2 we present the model and its analytical solution in the continuum limit. This solution is compared to the numerical simulations as the interaction law exponent is tuned from unity to large values. In section 3 we analyze the interaction of these shock waves with an impurity and display the energy distribution in the bead chain after the scattering with the impurity. A conclusion is given in section 4.

2 Theoretical results versus numerical simulations

The horizontal granular chain consists of N touching beads of equal sizes and masses. The repulsive interaction force between two adjacent beads under compression is written $F = k\delta^\alpha$ where δ is the overlap of the beads. For the exponent α equal to $\frac{3}{2}$ we have the Hertz law for perfectly spherical beads and the stiffness constant k can be expressed as a function of the spheres radii, the Young modulus and the Poisson ratio of the material. Here we let α vary from one to infinity considering beads with different geometries. The equation of motion for the displacement u_i of the bead i is given by

$$m\ddot{u}_i = k\delta_{i-1,i}^\alpha\theta(\delta_{i-1,i}) - k\delta_{i,i+1}^\alpha\theta(\delta_{i,i+1}) \quad 0 < i < N - 1 \quad (1)$$

In terms of the displacements of the beads $i - 1$ and $i + 1$ one can write

$$m\ddot{u}_i = k(u_{i-1} - u_i)^\alpha\theta(u_{i-1} - u_i) - k(u_i - u_{i+1})^\alpha\theta(u_i - u_{i+1}) \quad (2)$$

the Heaviside function having been introduced in order to have no tension forces.

This equation has been solved by Nesterenko [4] in the case of a shock perturbation by doing a long wavelength development. This approximation will be valid if the spatial extension of the wave generated by the shock is much greater than the size of a single bead. Assuming this we write u_i as $u(x, t)$. Moreover, since we are solving the equation for a wave in which the beads are compressed one can get rid of the Heaviside functions. The resulting equation is written

$$mu_{tt} = k \left(-au_x + \frac{a^2}{2}u_{xx} - \frac{a^3}{6}u_{xxx} + \frac{a^4}{24}u_{xxxx} \right)^\alpha - k \left(-au_x - \frac{a^2}{2}u_{xx} - \frac{a^3}{6}u_{xxx} - \frac{a^4}{24}u_{xxxx} \right)^\alpha \quad (3)$$

where a is the dimension of the bead and we developed $u(x+a)$ and $u(x-a)$ to fourth order. We then rewrite the equation

$$\frac{m}{k}u_{tt} = (-au_x)^\alpha \left[\left(1 - \frac{a}{2} \frac{u_{xx}}{u_x} + \frac{a^2}{6} \frac{u_{xxx}}{u_x} - \frac{a^3}{24} \frac{u_{xxxx}}{u_x}\right)^\alpha - \left(1 + \frac{a}{2} \frac{u_{xx}}{u_x} + \frac{a^2}{6} \frac{u_{xxx}}{u_x} + \frac{a^3}{24} \frac{u_{xxxx}}{u_x}\right)^\alpha \right], \quad (4)$$

$$-u_x > 0 \quad (5)$$

u_x being of order $\frac{u}{L}$ where L is the dimension of the pulse and expand the powers in Taylor series to the order $\frac{1}{L^3}$. We then obtain

$$\frac{m}{k}u_{tt} = a^\alpha \left(\alpha a (-u_x)^{\alpha-1} u_{xx} + \alpha \frac{a^3}{12} (-u_x)^{\alpha-1} u_{xxxx} - \alpha(\alpha-1) \frac{a^3}{6} \frac{u_{xx} u_{xxx}}{(-u_x)^{2-\alpha}} + \alpha(\alpha-1)(\alpha-2) \frac{a^3}{24} \frac{u_{xx}^3}{(-u_x)^{3-\alpha}} \right) \quad (6)$$

Looking for traveling wave solutions $u(\xi) \equiv u(x-Vt)$ with V being the speed of the wave, a longer calculation [4] gives us for the deformation

$$-u_x = \left(\frac{\alpha+1}{2} \frac{V^2}{c_\alpha^2} \right)^{\frac{1}{\alpha-1}} \left| \cos \left(\frac{\alpha-1}{\sqrt{\alpha(\alpha+1)}} \frac{\sqrt{6}}{a} \xi \right) \right|^{\frac{2}{\alpha-1}} \quad (7)$$

With

$$c_\alpha^2 = \frac{a^{\alpha+1} k}{m} \quad (8)$$

This periodic wave solution is singular since it violates the condition $-u_x > 0$ in eq.(5). We actually get the shock wave solution by imposing the argument of the cosines to vary in the interval $[-\frac{\pi}{2}(2k+1), \frac{\pi}{2}(2k+1)]$, $k \in \mathbb{Z}$. From the expression above we easily extract the wave speed V :

$$V = \left(\frac{2c_\alpha^2}{\alpha+1} \right)^{\frac{1}{\alpha+1}} v_{max}^{\frac{\alpha-1}{\alpha+1}} \quad (9)$$

v_{max} being the maximum of the velocity pulse.

The accuracy of this analytical approximation has been tested numerically with a Gear fifth order predictor-corrector algorithm on a horizontal chain of 200 beads with free boundary conditions. A shock perturbation is imposed on the chain by giving the first bead a $5m.s^{-1}$ speed at zero time. We choose beads of mass $m = 1g$ and stiffness $k = 10^7 N.m^{-1}$. We first looked at the shape of the deformation profile of the bead number 100 as function of time and compared

it with the shape given by the expression (7) for different values of α . We displayed in fig.(1), fig.(2) and fig.(3) the superposition of numerical and analytical curves for α equal to 1.2, 1.5 and 1.7. One easily sees on these curves that the analytical results are rather good for low values of α ($\alpha > 1$) showing discrepancies when α is increased. Actually, the tails of the deformations curves are much longer than the ones given by equation (7). If the value of α is increased to higher values the numerical and analytical results become completely different as one can see in fig.(4) where we took α equal to 10.0. Other discrepancies can be found if α is taken in the neighborhood of unity. It can be seen in fig.(5) that the deformation curve on the bead number 100 is not symmetric when α is taken equal to 1.01. This non-symmetric shape actually evolves to a symmetric one as the pulse propagate. We simulated a chain of 3000 beads and considered the deformation of the bead number 2000 : the pulse has the soliton shape given by equation (7) (fig.(6)). The pulse has actually to propagate over 2000 beads before reaching its solitonic regime predicted by (7). In fact, there is a cross-over between a nonlinearity-dominated regime and a solitonic regime where dispersion is balanced by nonlinearity. The non-linearity dominated regime corresponds to a transient where the amplitude of the pulse decreases slowly in time before reaching a constant value, i.e, the solitonic regime. At the same time the width of the pulse increases also reaching a stationary value. Moreover the shape of the pulse evolves continuously from a non-symmetric one to a symmetric one. The time of the transient obviously increases as we decrease α (if we take $\alpha = 1.004$ the pulse has to propagate over 15000 beads before reaching its stationary value). This cross-over behavior can be understood by looking at equation (6) for α close to one. We can rewrite this equation with a small parameter ϵ where $\alpha = 1 + \epsilon$:

$$\frac{m}{k}u_{tt} = a^{2+\epsilon}(-u_x)^\epsilon \left(u_{xx} + \frac{a^2}{12}u_{xxxx} \right) \quad (10)$$

If we consider $(-u_x)^\epsilon$ constant equal to one we obtain the long wavelength equation for the linear springs chain which is the same as the simple wave equation up to a dispersive term, the fourth order derivate of the displacement. It has been shown [5, 6] that the velocity solution of this equation is not a soliton but a non-symmetric self-similar wave of decreasing amplitude and increasing width, the amplitude going to zero and the width going to infinity as time goes to infinity. For α close to one the non-linearity $(-u_x)^\epsilon$ vary slowly and the time for it to balance the action of the dispersive four order term increases as ϵ goes to zero. We can actually calculate how the amplitude and the width of the velocity pulse vary with epsilon. The velocity of a bead is given by eq.(7) up to the factor V . Replacing α with $\epsilon + 1$ we get :

$$v = A \left| \cos \left(\frac{\sqrt{6}\epsilon}{a\sqrt{(\epsilon+1)(\epsilon+2)}}\xi \right) \right|^{\frac{2}{\epsilon}} \quad (11)$$

where

$$A = \left(\frac{\epsilon + 2}{2} \frac{V^{\epsilon+2}}{c_{\epsilon+1}^2} \right)^{\frac{1}{\epsilon}} \quad (12)$$

We then write eq.(11) in an exponential form and expand its argument in a Taylor series keeping the lower order term :

$$v = A \exp \left(- \frac{6\epsilon}{a^2(\epsilon + 1)(\epsilon + 2)} \xi^2 \right) \quad (13)$$

The solution of eq.(6) is then approximated by a Gaussian for α close to unity. According to the properties of Gaussian distributions the width w of the solitary wave follows the scaling law $w \propto \epsilon^{-\frac{1}{2}}$, i.e :

$$w \propto (\alpha - 1)^{-\frac{1}{2}} \quad (14)$$

For $\alpha = 1$ we recover the result of [5, 6] where the width of the wave was found to diverge as time goes to infinity. We checked numerically the accuracy of this scaling relation and found a good agreement (see Fig.(7)). A second scaling relation can be obtained by using the conservation of the kinetic energy in the wave since the beads following the wave have negligible velocities. It follows that the product $v_{max}^2 w$ remains constant. Hence,

$$v_{max} \propto (\alpha - 1)^{\frac{1}{4}} \quad (15)$$

We again recover the result of [5, 6] where the velocity amplitude was found to go to zero as time goes to infinity. We displayed in Fig.(8) the value of the final velocity amplitude v_{max} when α is varied in the neighborhood of one and found again a good agreement with the obtained scaling relation. These two scaling laws show that the transition between the self-similar regime $\alpha = 1$ to the solitonic regime $\alpha > 1$ is actually continuous, the value $\alpha = 1$ being not singular.

3 Collision of a shock wave with an impurity

After having considered the propagation of a single solitary wave in a chain of equal masses we want to present what are the consequences of the introduction of a single impurity on the stability of a shock wave. For that, we consider a chain of 1000 beads, the bead 500 being replaced by an impurity. By impurity we mean a bead whose mass is larger or smaller than the mass of its neighbors. Different behavior arises as we introduce a light or an heavy impurity. Besides, we also have to take into account the value α of the interaction law exponent. The simplest way of looking at what happens when a shock generated on the left end of the chain scatters the impurity is to compute the velocity and the displacement of the

beads after the collision. Fig.(9) displays velocities for a light impurity and an exponent α equal to 1.5. The leading wave corresponds to the shock wave which is followed by an increasing number of secondary solitary waves with decreasing amplitudes generated at the impurity position. A symmetric pattern arises in the opposite direction since solitary waves with negative velocities and almost same amplitudes as the previous ones propagate. The wave speed of the incident shock is modified after the collision since its amplitude decreases providing with energy the impurity which can then generate new waves. The corresponding displacement profile is displayed on Fig.(10) where the pulses are now replaced by the squared front waves characteristics of shock waves. In order to better understand the phenomenon we looked at the spatio-temporal pattern exhibited by the scattering. In Fig.(11) one can see black straight lines defining compression waves whereas white zones mean beads are at touching. The secondary pulses are created at the impurity position and after a transient displayed by thin curved black lines near the impurity location they propagate with a constant velocity reaching then a stationary regime. The wave speed of these pulses are decreasing as new pulses are created as one can see by looking at the slopes of the black lines. It agrees with the display of waves with decreasing amplitudes in Fig.(9). From these observations we can conclude that the light impurity acts as a wave source. In order to understand the behavior of this source we computed the displacement of the impurity as function of time after the scattering. Fig.(12) clearly shows that the impurity oscillates around an equilibrium position. These oscillations are zig-zag shaped showing that the impurity moves with a constant velocity between two shocks with its left and right neighbors. This velocity decreases in time (lower slopes of the oscillations) since the impurity transfers energy to its neighbors at each shock creating new pulses. Although we chose special values for the impurity mass and the interaction law exponent the same behavior is observed if we maintain the impurity mass lower than the chain masses and the interaction exponent greater than one.

If we now turn to the case of an heavy impurity we observe a very different physical picture. In Fig.(13) we displayed the velocity of the beads for an impurity mass greater than beads chain mass, the interaction exponent remaining equal to 1.5. The collision generates many pulses of decreasing amplitudes behind the impurity, these pulses being very close to each other. Moving in the opposite direction one can see one pulse of large amplitude. This pattern is not symmetric as in the case of a light bead and a different physical process seems to be involved. We can better understand what happened by looking at the spatio-temporal pattern of contacts displayed in Fig.(14). After collision the bead chain is halved as it is shown by the white vertical line separating two black areas meaning compression between beads. The impurity has actually been given a shift to the right when it collided with the shock wave. Instead of bouncing back the impurity sticks and there is the formation of a compression chain. The beads following the impurity don't remain homogeneously compressed and there is a fragmentation

of the incident pulse giving rise to many pulses corresponding to the straight lines of decreasing slopes on the spatio-temporal pattern. These lines obviously correspond to pulses of decreasing amplitude in Fig.(13). Between these pulses the beads remain at rest just touching their nearest neighbor. Other compression areas appear on the left side. The straight line of larger slope is the main reflected wave. A growing compression zone moving at constant velocity follows this pulse. After some times this area also begins to fragment into new pulses as one can see from the black straight lines appearing at the front. These new compression pulses are not visible on the velocity profile since their amplitude is too low. This spatio-temporal pattern allows us to say that the collision of a shock wave with an heavy impurity make it fragment into solitary waves of decreasing amplitudes. This is not what happens when we introduce a light impurity since the shock excites the impurity. To our knowledge, the scattering with an heavy mass is the simplest way to make the solitary wave unstable. As in the previous case, although we took $10g$ for the impurity mass and 1.5 for the interaction exponent the obtained pattern remains unchanged as these two parameters are tuned.

The number of fragmented pulses actually increases with the mass of the impurity. To show it we considered a chain of equal masses with a bead of larger mass at its beginning. In the case of a bead having the same mass we know that the perturbation of the first bead by giving it a finite velocity at zero time will produce a single pulse. As we increase the mass of this first bead an increasing number of pulses appear by the same process as described previously. We plotted the corresponding velocity profiles for two different values of the first bead mass in Fig.(15) and Fig.(16).

We also looked at the energy distribution in the bead chain as function of the mass of the impurity and of the value of the force interaction exponent. Fig.(17) shows the ratio of the reflected energy at the impurity location over the total energy in the chain. The reflected energy is defined as the energy contained in the first half of the bead chain after scattering. This energy is not stationary immediately after wave reflection and we have to wait the time for it to reach a stationary value. The impurity mass varies between $0.6g$ and $5g$ and α takes values between 1.01 and 5 . One easily sees that the amount of reflected energy increases as the mass difference increases. This amount also increases with α if the the impurity mass is greater than a value located between $1.5g$ and $2g$. Below this value the curves cross each others at different values of the impurity mass. Below the crossing it is the lowest value of the two exponents which gives the greater amount of reflected energy. If we now consider the ratio of reflected energy over transmitted energy in Fig.(18) we observe similar variations as previously. Moreover the ratios remain lower than unity meaning that the amount of reflected energy is always lower than the amount of transmitted energy in the impurity mass interval considered.

4 Conclusion

We investigated the problem of a shock propagating in a non-loaded horizontal granular chain with a general beads interaction force $F \propto \delta^\alpha$, $\alpha > 1$. We compared our numerical simulations with previous analytical results obtained in the long wavelength approximation [4]. For values of α close to unity we found a cross-over between a non-linearity dominated regime and a solitonic one corresponding to the long wavelength approximation. The latter regime is reached after a time which increases and tends to infinity as one tunes α to unity. It was then shown that the transition between the $\alpha = 1$ [5, 6] (self-similar) regime to the $\alpha > 1$ regime is continuous. In the case of large values of α we observed discrepancies between numerical simulations and analytical results. As α increases beyond 1.2 tails in the deformation curves separate. When α reaches the value of 1.7 the analytical result given for the deformation curve is already not reliable. In the limit of very large values of α the deformation curve takes a triangular shape totally inconsistent with the one given by the theoretical analysis.

We then studied the interaction of these solitonic shock waves with an impurity mass placed in the middle of the bead chain. We first considered light impurities. The scattering of the shock with the impurity actually excites it in an oscillatory ballistic damped motion. The impurity acts as a wave source emitting solitary waves of decreasing amplitude in both directions. If we place an heavy impurity in the bead chain we observe a completely different pattern. The impurity is no more excited but sticks its next neighbor splitting the bead chain in two parts. The chain corresponding to the transmitted wave supports no more solitonic propagation and we have an instability displayed by the fragmentation of the transmitted wave into waves of decreasing amplitudes. On the other half of the chain a reflected stable solitonic wave propagates followed by a growing unstable fragmented front appearing at the impurity location. The physics involved in this case is much more complicated and deserves further investigations.

References

- [1] V. F. Nesterenko, *Prikl. Mekh. Tekh. Fiz.* **5** 136-148 (1983).
- [2] A. N. Lazaridi and V. F. Nesterenko, *Prikl. Mekh. Tekh. Fiz.* **3**, 115-118 (1985).
- [3] C. Coste, E. Falcon and S. Fauve, *Phys. Rev. E* **56**, 6104 (1997).
- [4] V. F. Nesterenko, *Journal de Physique IV* **4**, C8-729 (1994)
- [5] E. Hascoët, H. Herrmann and V. Loreto, *Phys. Rev. E* **59**, 3202 (1999)
- [6] E. J. Hinch and S. Saint-Jean, *Proc. R. Soc. Lond. A* **455**, 3201-3220 (1999)

- [7] S. Sen, M. Manciu and J. D. Wright, *Phys. Rev. E* **57**, 2386 (1998).
- [8] J. Hong, J.-Y. Ji and H. Kim, *Phys. Rev. Lett.* **82**, 3058 (1999).

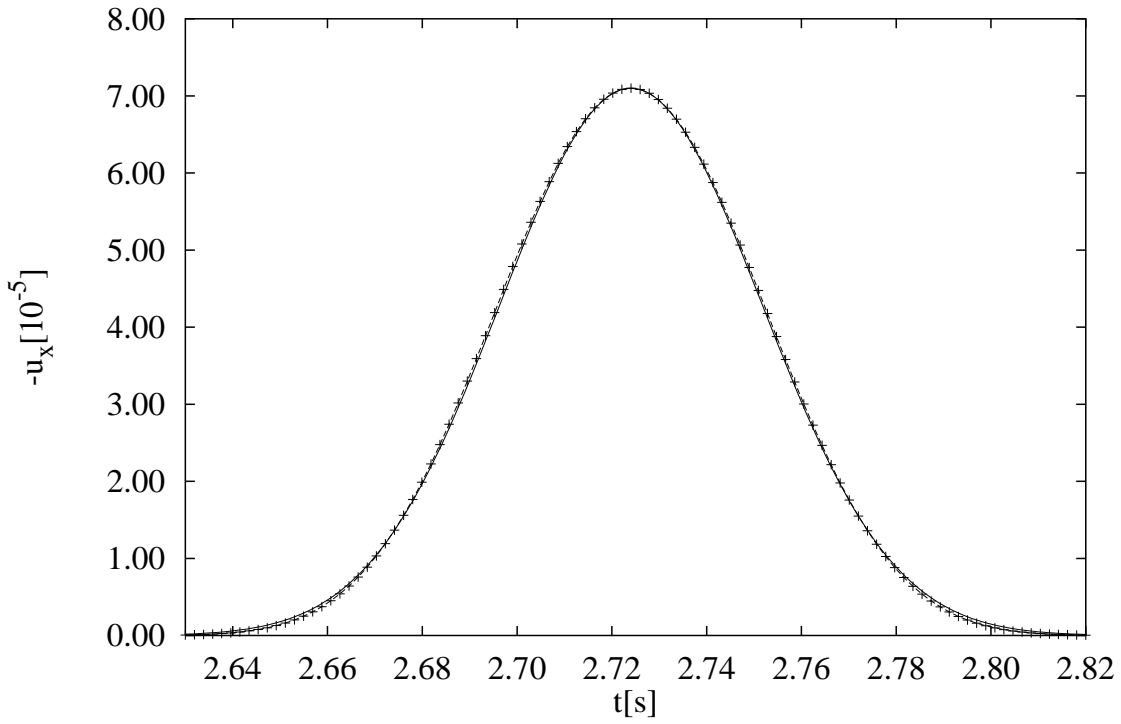


Figure 1: Deformation curves of the bead number 100 in a chain of 200 beads, the force exponent being equal to 1.2. There is very good agreement between numerical and theoretical results. The crossed curve from the analytical result eq.(7) superimposes the plain line curve from the numerical simulation. The crossed curve obviously correspond to a single oscillation of the periodic solution eq.(7).

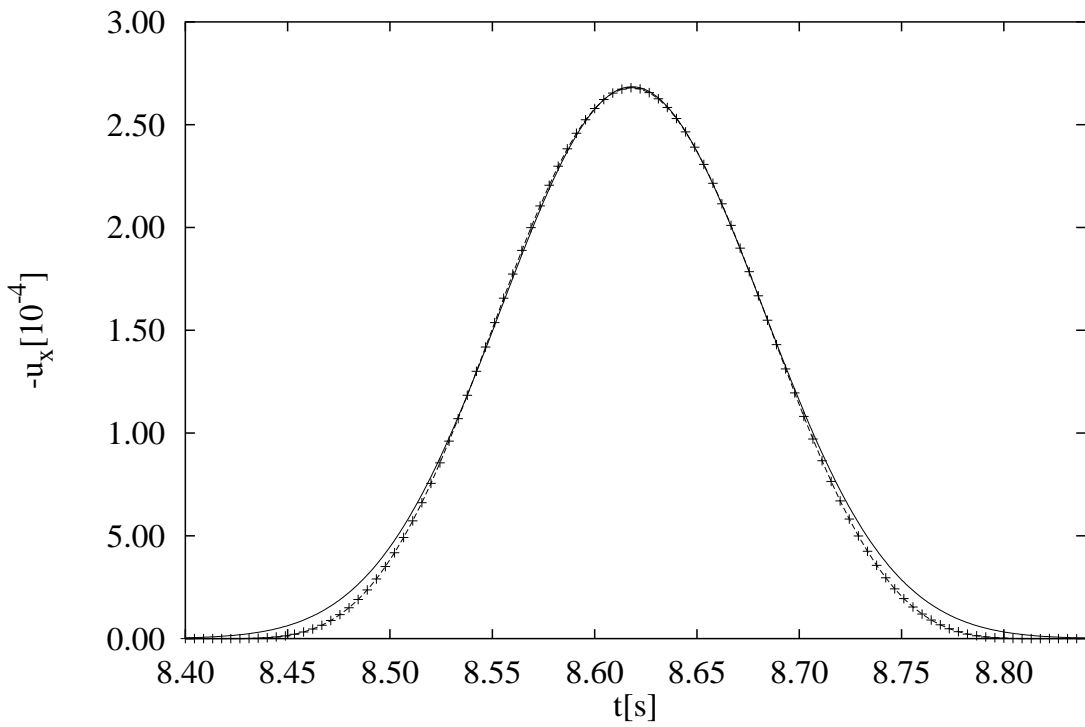


Figure 2: Deformation curves when $\alpha = 1.5$. Discrepancies between numerical and theoretical results appear at the curves tails. The crossed tails of the analytical result remain below the real tails of the numerical simulation.

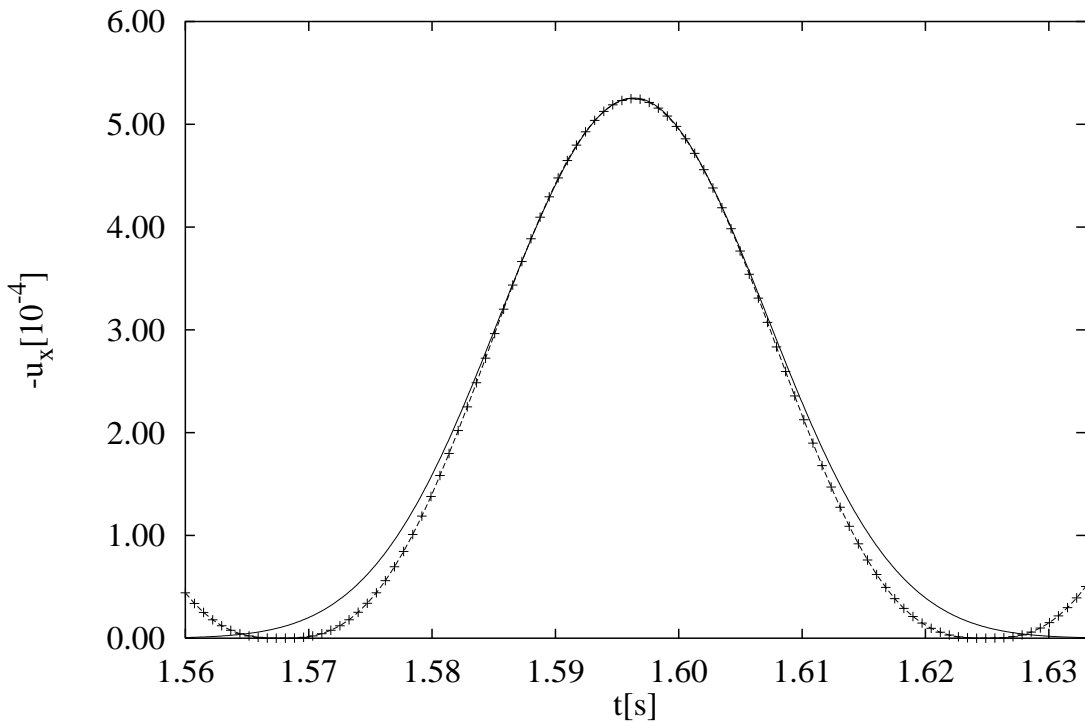


Figure 3: Deformation curves when $\alpha = 1.7$. The increase in α increases the deviation of the curves at the tails. The oscillating character of the analytical result is displayed at the corners of the plot where one can see the end of the previous oscillation of the non-linear periodic solution on left and the beginning of its next oscillation on right.

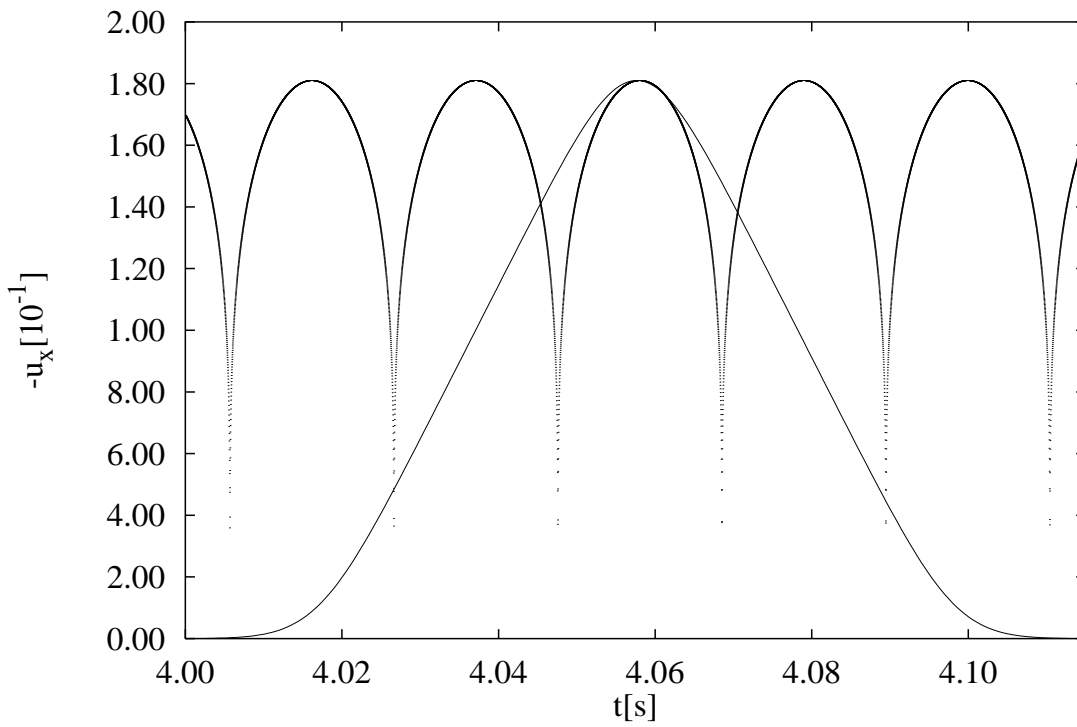


Figure 4: Deformation curves when $\alpha = 10$. There is no agreement between analytical and numerical results. The true deformation has a triangular shape while the analytical curve display a periodic parabola shape.

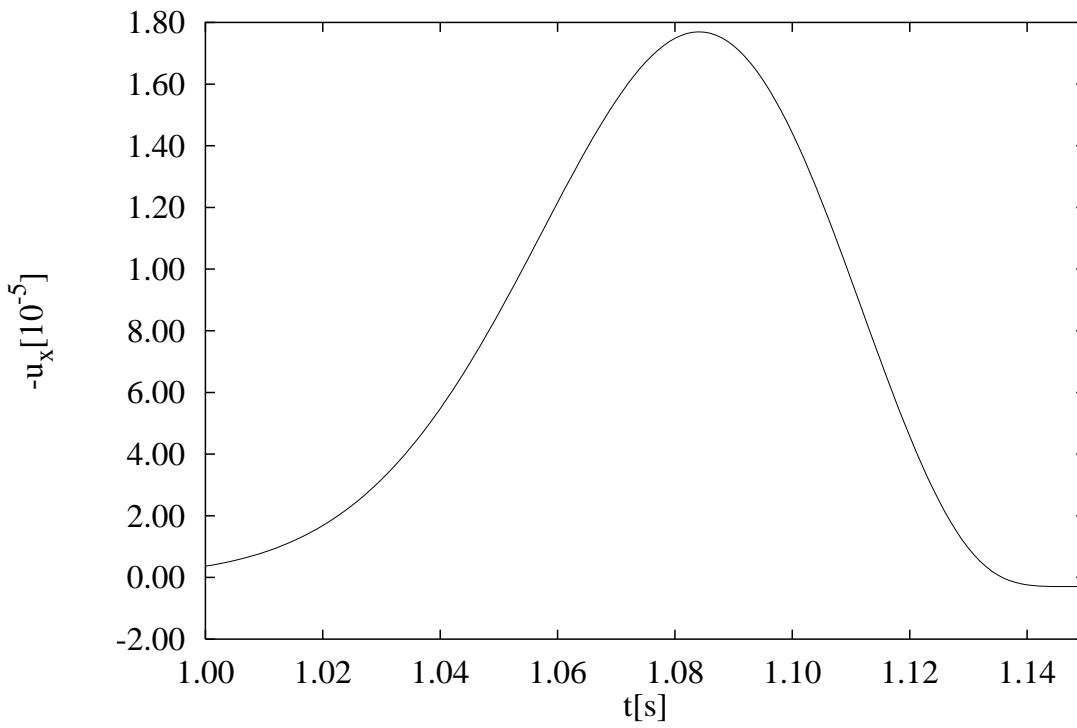


Figure 5: Deformation curve when $\alpha = 1.01$ for bead number 100. The pulse is not symmetric. We are in the non-linearity dominated regime.

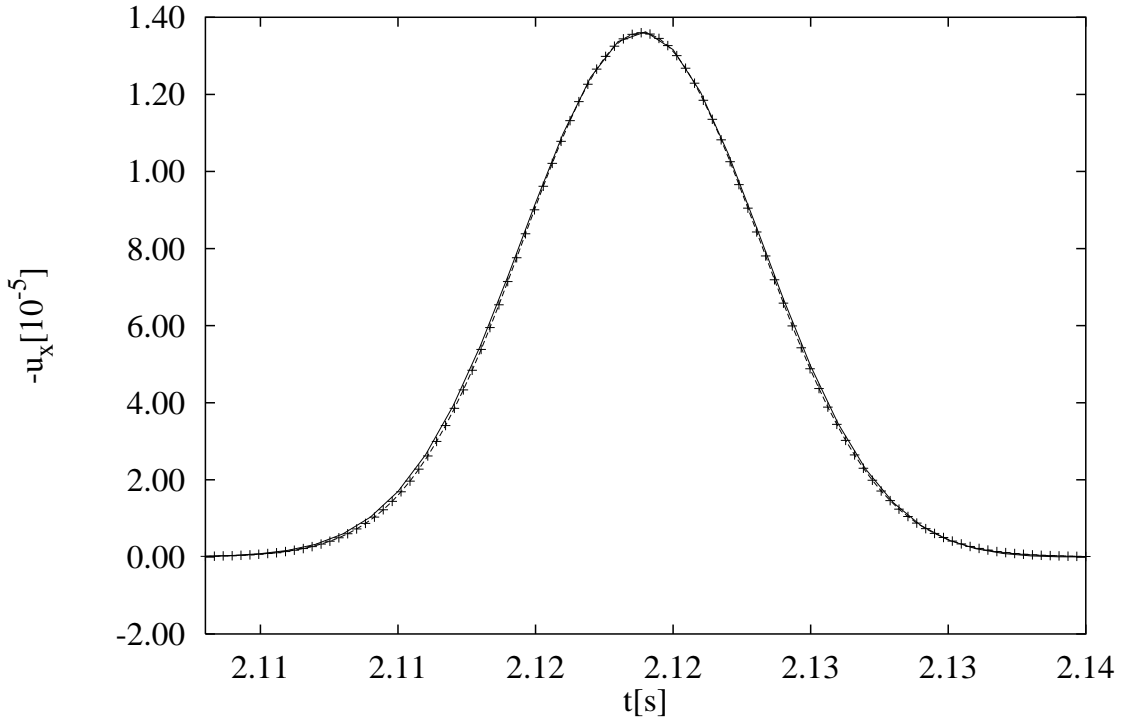


Figure 6: Deformation curves when $\alpha = 1.01$ for bead number 2000 of a bead chain of 3000 beads. The pulse reached its stationary soliton shape given by eq.(7) and the numerical and analytical curves superimpose.

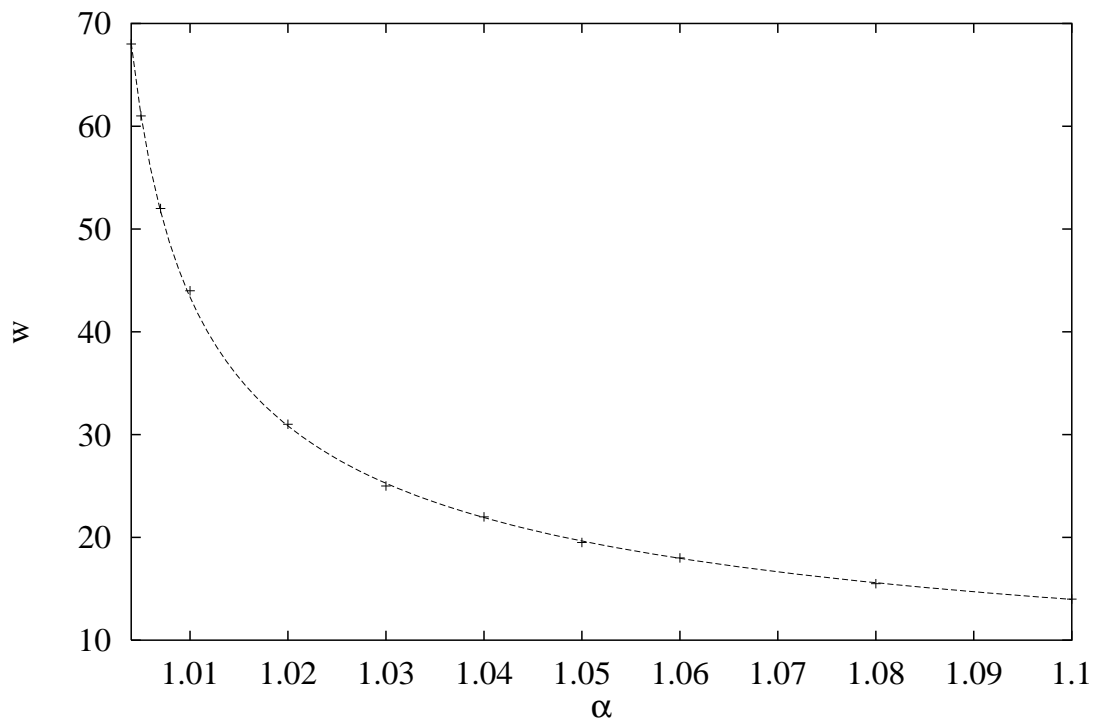


Figure 7: Plot of the width of the pulse as function of α when α is close to unity. The dashed line displays the corresponding power law : $w \propto (\alpha - 1)^{-0.492}$.

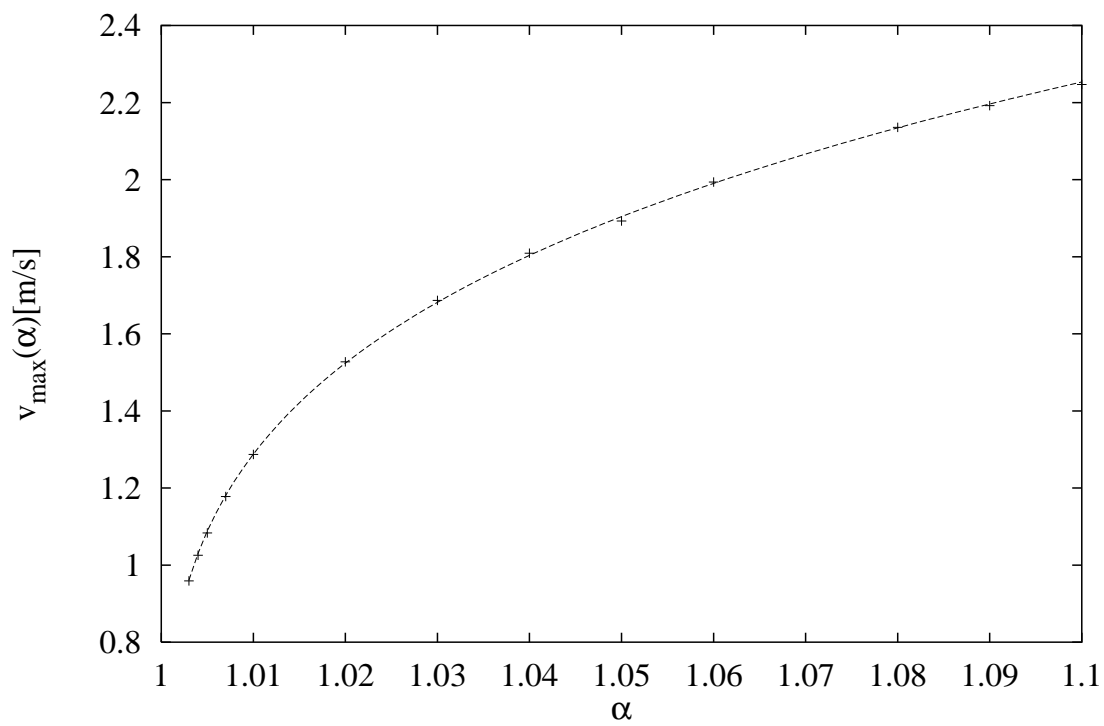


Figure 8: Plot of the velocity pulse amplitude as function of α when α is close to unity. The dashed line displays the corresponding power law : $v_{max} \propto (\alpha - 1)^{0.243}$.

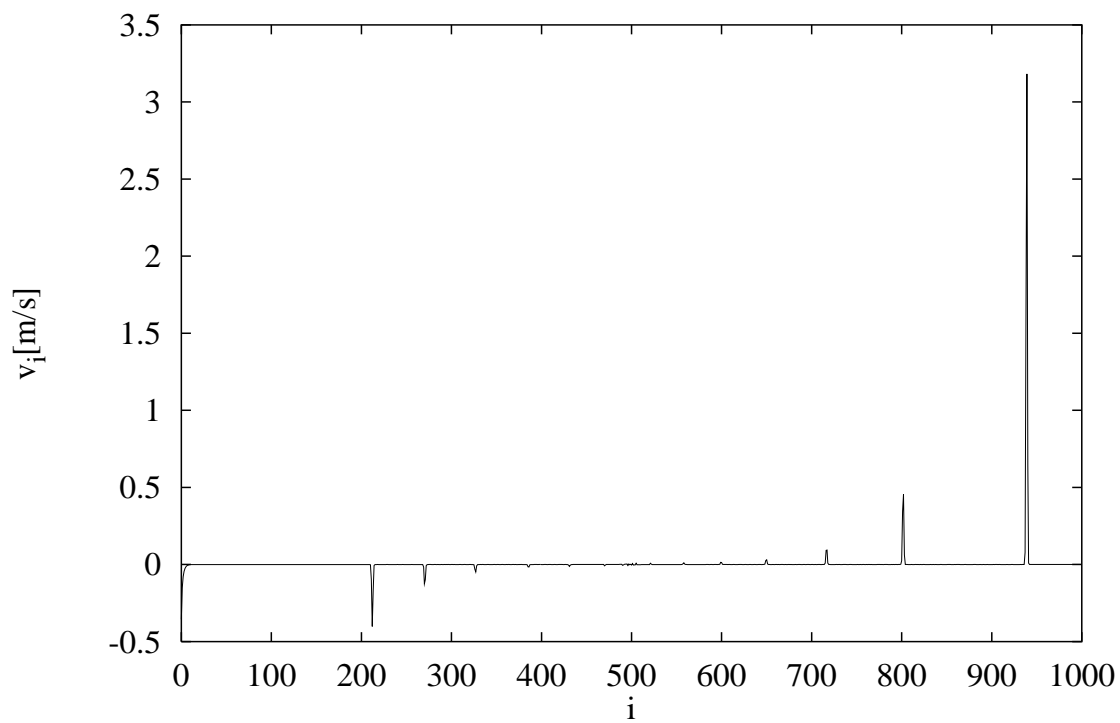


Figure 9: Velocities of the 1000 beads after the scattering of the shock with a light impurity of mass $m_i = 0.6g$, the normal mass being $m = 1g$. The force interaction exponent is $\alpha = 1.5$. Solitons are emitted at the impurity location in forward and backward directions.

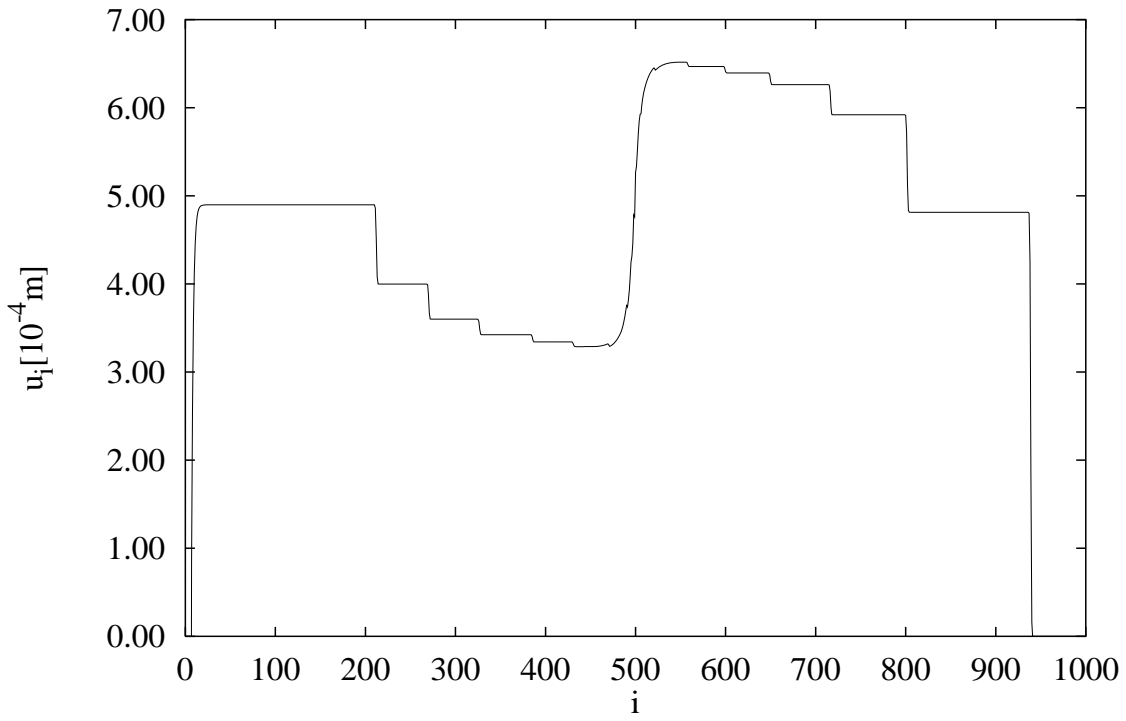


Figure 10: Displacement profile corresponding to the velocity profile.

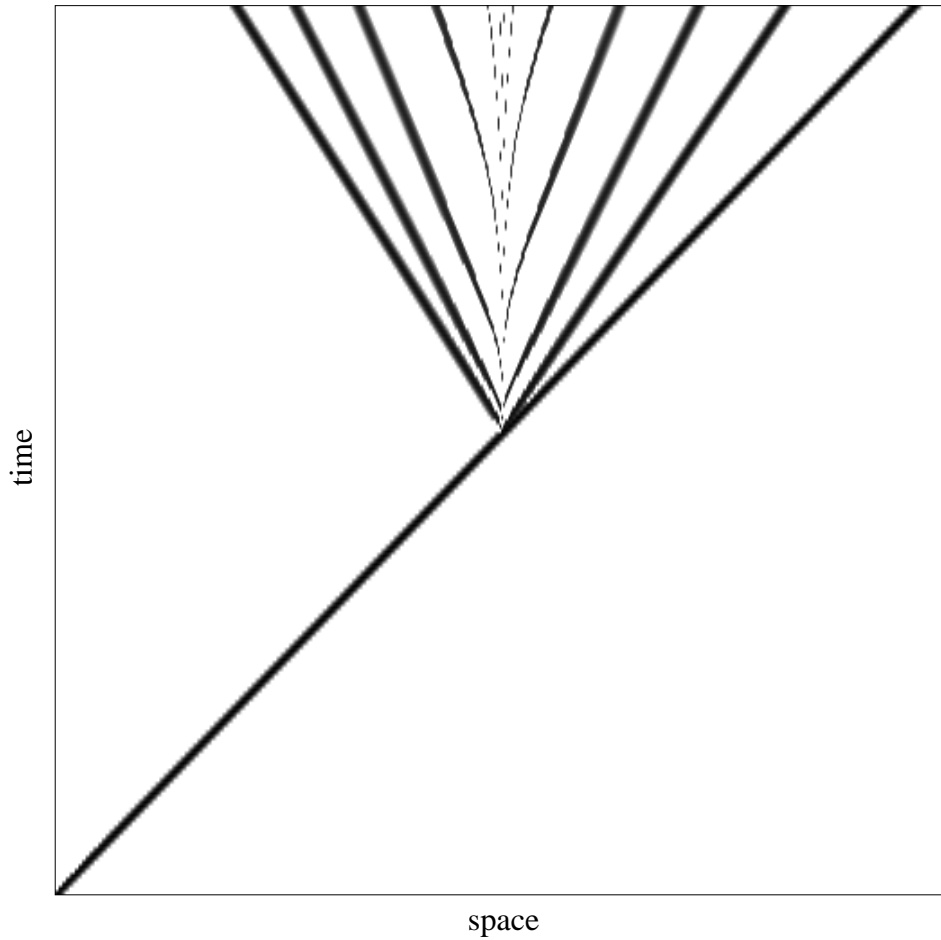


Figure 11: Spatio-temporal evolution of beads contacts for the collision with a light impurity of mass $m_i = 0.6g$. A black dot means that two beads are in compression while a white dot means that they are at touching. α is equal to 1.5. Black straight lines correspond to compression pulses.

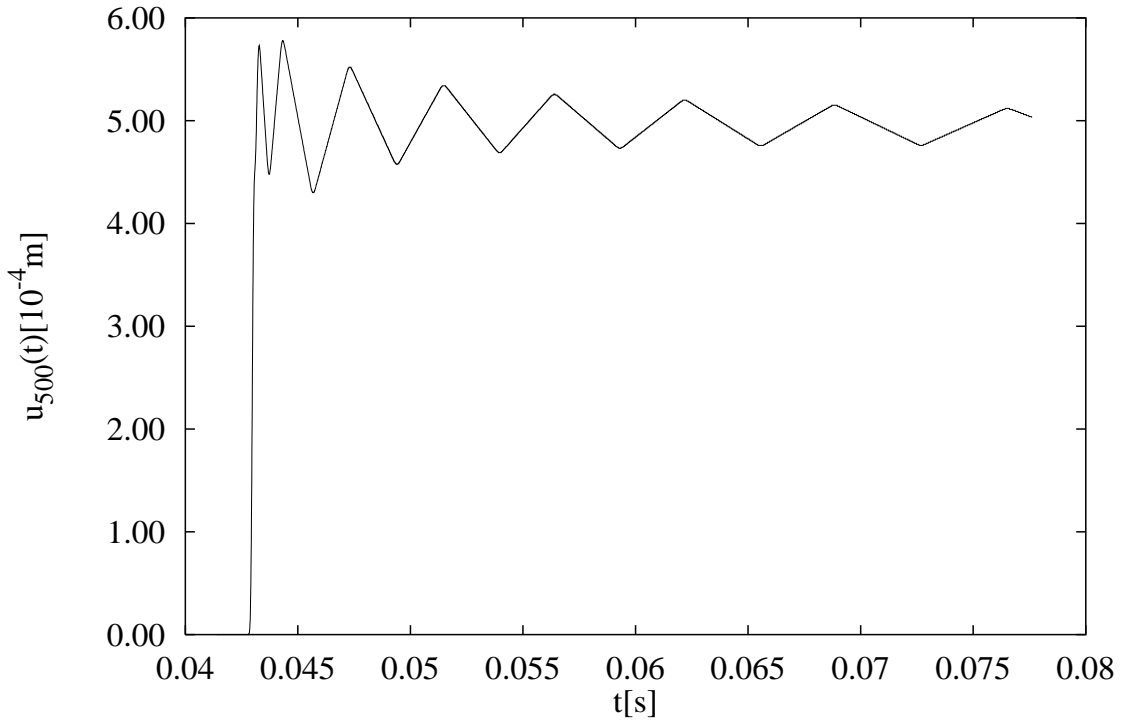


Figure 12: Displacement of the impurity located at the position 500 in function of time for $m_i = 0.6g$ and $\alpha = 1.5$. The light impurity oscillates in a damped ballistic motion showed by the zig-zag shape of the curve.

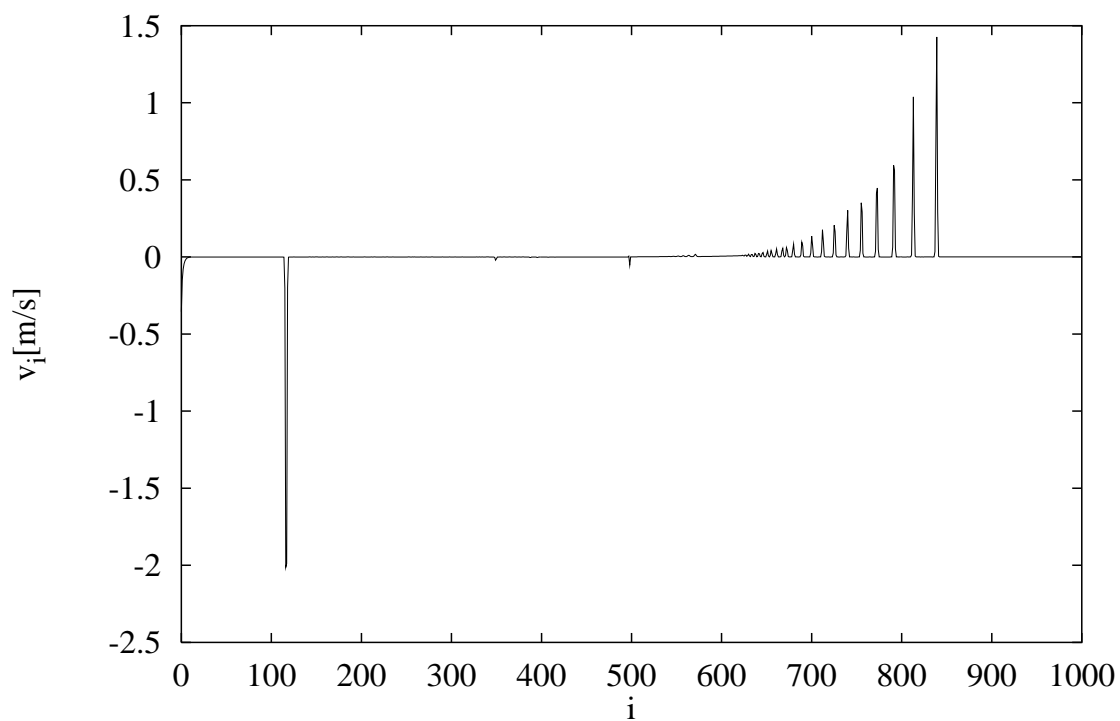


Figure 13: Velocities of the 1000 beads after the scattering of the shock with a heavy impurity of mass $m_i = 10g$ ($\alpha = 1.5$). The transmitted solitary wave fragments into many solitary waves of decreasing amplitudes. The major reflected part is displayed by a single pulse.

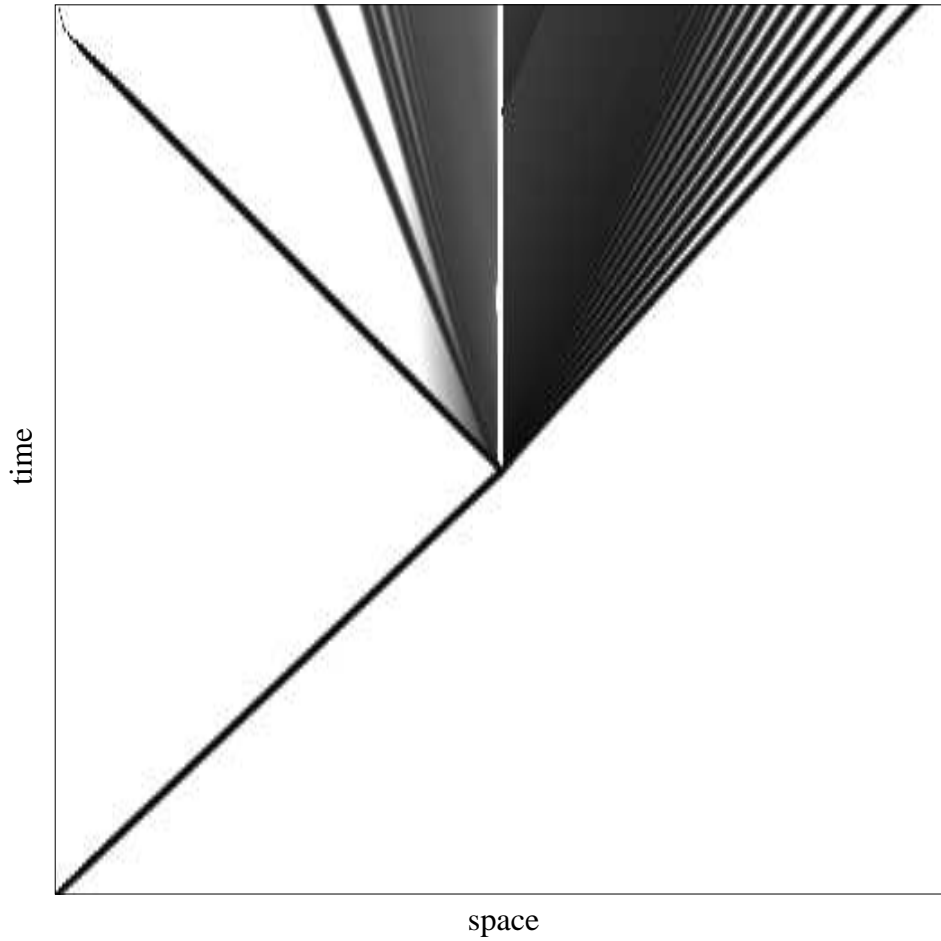


Figure 14: Spatio-temporal evolution of beads contacts for the collision with an heavy impurity of mass $m_i = 10g$ ($\alpha = 1.5$). In addition to the transmitted fragmented front one can see a second fragmenting front following the reflected wave.

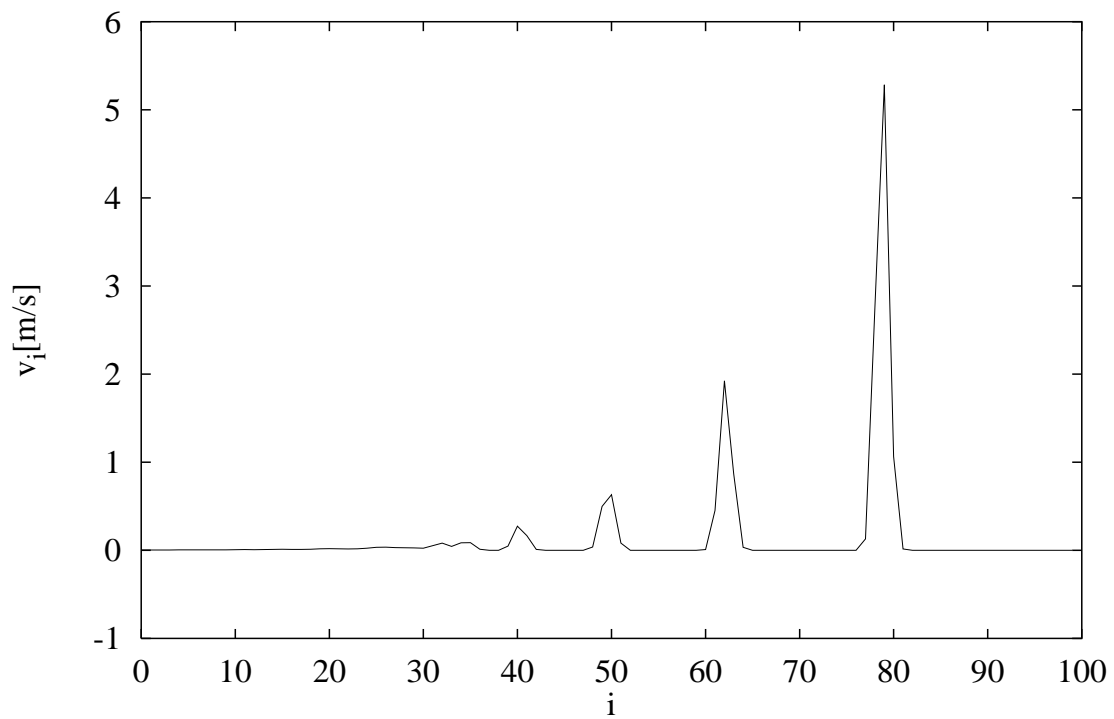


Figure 15: Velocities in a 100 beads chain when it is perturbed with an heavy mass of $3g$ ($\alpha = 1.5$) with initial velocity of $5m.s^{-1}$. Instead of having a single soliton as it is the case for a homogeneous chain many pulses of decreasing amplitudes are propagating.

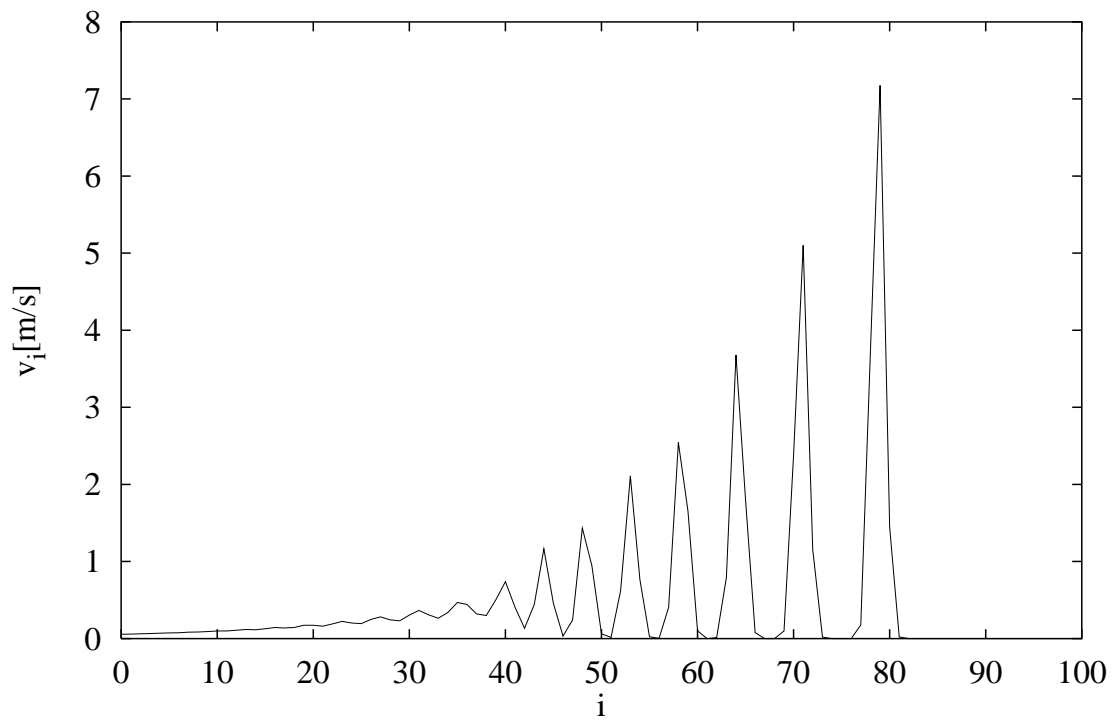


Figure 16: Velocities in a 100 beads chain when it is perturbed with an heavy mass of $10g$ ($\alpha = 1.5$) with initial velocity of $5m.s^{-1}$. As the mass of the first bead is increased the number of emitted pulses grows.

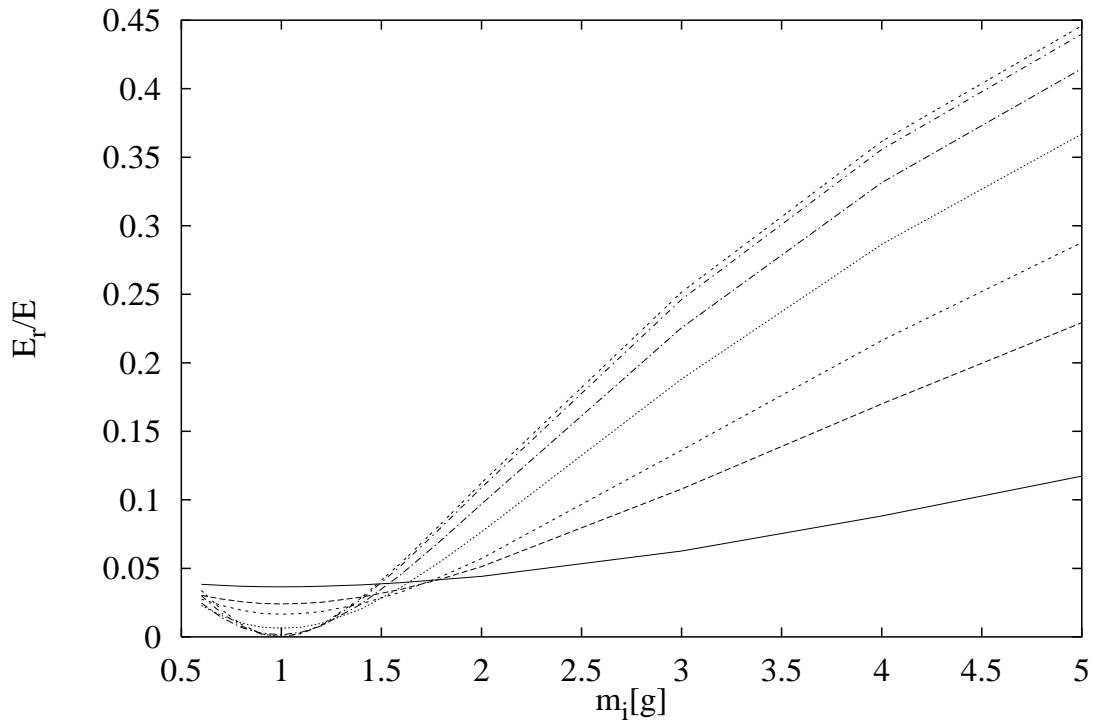


Figure 17: Ratios of the reflected energy over the total energy of the bead chain for different values of α . Going from the upper right curve to the lower right curve α takes the values 5, 3, 2, 1.5, 1.2, 1.1 and 1.01. When m_i is greater than a value between 1.5 and 2 the energy ratio increases with α . Below this threshold we have a more complicated pattern in which curves cross each others at different locations.

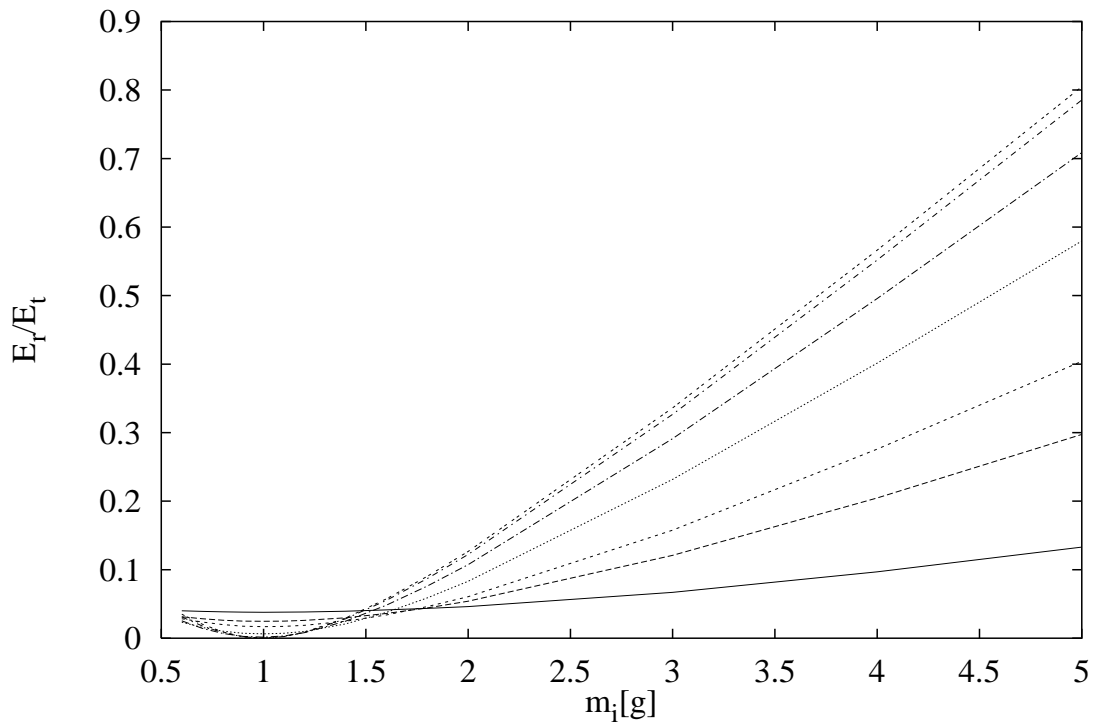


Figure 18: Ratios of the reflected energy over the transmitted energy. Going from the upper right curve to the lower right curve α takes the values 5, 3, 2, 1.5, 1.2, 1.1 and 1.01. A similar pattern as the one for the reflected energy over the total energy is obtained. The part of reflected energy remains lower than the part of transmitted energy in the impurity mass considered.